PHYSIOLOGY 22: 47–55, 2007; 10.1152/physiol.00036.2006

Optical Recording of Action Potentials and Other Discrete Physiological Events: A Perspective from Signal Detection Theory

Lucas Sjulson
and Gero Miesenböck
Department of Cell Biology,
Yale University School of Medicine,
New Haven, Connecticut
lukesjulson@gmail.com

Optical imaging of physiological events in real time can yield insights into biological function that would be difficult to obtain by other experimental means. However, the detection of all-or-none events, such as action potentials or vesicle fusion events, in noisy single-trial data often requires a careful balance of tradeoffs. The analysis of such experiments, as well as the design of optical reporters and instrumentation for them, is aided by an understanding of the principles of signal detection. This review illustrates these principles, using as an example action potential recording with optical voltage reporters.

Many physiologists rely on optical techniques for measuring spatially and temporally resolved physiological signals in living cells. The signals typically originate from synthetic or biosynthetic sensor molecules that report changes in physiological variables as changes in fluorescence intensity. Such sensors now exist for numerous parameters and events, such as the concentrations of Ca^{2+} and various other second messengers, membrane potential, pH, and vesicle release (12, 27, 28, 50). Although wide-field microscopy remains the most commonly employed method for detecting fluorescence in living cells, its performance is often poor in thick tissue, where background fluorescence from focal planes above and below the region of interest can severely degrade the signal-to-noise ratio. To overcome this problem, different forms of laser scanning microscopy have been developed that possess the capacity to excite fluorescence in (or collect fluorescence from) only a single focal plane, thereby eliminating out-of-focus light. However, scanning microscopy in itself carries a price of massively reduced photon counts, which decreases the signal-to-noise ratio and defeats some of the advantages of optical sectioning.

The choice of optimal imaging strategies for a given biological application thus requires a careful balance of tradeoffs. This is particularly true for the detection of all-or-none events, such as action potentials (APs) or vesicle fusion events (6, 26), in noisy single-trial data, where across-trial averaging cannot be used. The analysis of such experiments, as well as the design of optical reporters and instrumentation, requires an understanding of the basic principles of signal detection. This review illustrates these principles, using as an example the detection of APs with optical voltage reporters.

Optical Voltage Reporters

Recording APs from a large percentage of neurons in intact neural circuits with high temporal resolution is a largely unrealized goal in experimental neurophysiology. Imaging membrane potential with optical voltage reporters is one of the techniques promising to break through this barrier. Voltage reporters are sensitive to the cellular membrane potential, an electric field generated across the plasma membrane by the combination of ion-selective permeation and ionic concentration gradients. During an AP, changes in ionic permeability briefly reverse the polarity of the membrane potential. Although the characteristic AP waveform is in reality more complex, we approximate an AP as a square pulse lasting 1 ms for the purposes of our discussion.

Since the electric field is localized to the plasma membrane, voltage reporters require a probe that sits in the plasma membrane itself. The change in membrane potential during an AP affects the probe molecule in a way that alters an optically observable parameter, such as fluorescence. All published voltage reporters with fast kinetics fall into four classes: fast voltage-sensitive dyes (VSDs), two-component VSDs, hybrid GFP-dye systems, and fusions of GFP with ion channels.

Fast VSDs (FIGURE 1A) were the first voltage reporters developed by Cohen and colleagues (12, 40). VSDs partition into one leaflet of the plasma membrane, where they are influenced by the membrane electric field. The three major mechanisms of fluorescence modulation by membrane voltage are believed to be potential-dependent spectral shifts (electrochromism), dipole reorientation, and alterations of monomer-dimer equilibria (15, 17, 25, 47).

1548-9213/05 8.00

Two-component dye systems (FIGURE 1B) were first developed by Gonzalez and Tsien (19, 20). In two-component VSDs, a stationary dye is anchored to one face of the plasma membrane, while a mobile dye redistributes between the inner and outer membrane leaflets in a voltage-dependent manner. The change in the distribution of distances between stationary and mobile dye molecules leads to changes in fluorescence resonance energy transfer (FRET) efficiency and corresponding changes in fluorescence.

Hybrid GFP-dye systems (FIGURE 1C) are analogous to the two-component VSD systems, except that the stationary dye is replaced by a GFP anchored to the cytoplasmic face of the plasma membrane. This design was also pioneered by the Tsien group (45). Recently, the approach has been extended in the hybrid voltage sensor (hVOS) system (10), in which a nonfluorescent mobile dye quenches the fluorescence of the membrane-bound GFP.

Voltage reporters based on GFP-channel fusions (FIGURE 1D) were introduced by Siegel and Isacoff with the development of FlaSh, or "Fluorescent Shaker," a fusion of GFP with the Shaker potassium channel (43). Voltage-gated cation channels undergo a series of conformational changes with membrane voltage and in fact underlie the AP itself. Although the mechanism of fluorescence modulation is not clear, GFP-channel fusions operate according to the principle that normal conformational changes of the channel are translated to changes in GFP fluorescence. Several GFP-channel fusions exist: FlaSh, VSFP1 (38), and SPARC (3), as well as several modified versions of FlaSh (21).

Wide-Field vs. Laser Scanning Microscopy

Early successes with voltage reporters involved wide-field imaging of squid axons (13) and certain favorable invertebrate preparations (40) stained with synthetic VSDs. However, extension of VSD imaging to intact mammalian tissue has often proved problematic. The primary reasons for this difficulty are twofold. First, bulk-applied synthetic dyes label not only the cells of interest but rather stain all neuronal and nonneuronal cell membranes in the preparation indiscriminately. Second, wide-field imaging cannot extract the signals of interest selectively but rather captures fluorescence also from every focal plane above and below the cells of interest. These two factors (indiscriminate labeling and detection of out-of-focus fluorescence) work together to decrease the signal-to-noise ratio so severely that single-trial imaging with single-cell resolution generally becomes impossible, with few notable exceptions (30).

Biosynthetic voltage reporters potentially solve the problem of indiscriminate labeling (see below), whereas laser scanning microscopy solves the problem of detecting out-of-focus fluorescence by optical sectioning, or selectively imaging a single plane in the specimen. There are three common forms of laser scanning microscopy with optical sectioning capability: confocal, two-photon (14), and second harmonic generation (SHG) microscopy (8). In confocal microscopy, a pinhole rejects out-of-focal plane light, whereas in two-photon and SHG microscopy, emission light is generated only at the point of focus.

Despite superior depth penetration and resolution in thick tissue, laser scanning microscopy introduces two serious technical difficulties for recording short-duration optical events, such as APs. First, because the beam must be scanned point by point over the specimen, image acquisition is much slower than wide-field imaging: frame rates for typical laser scanning microscopes are in the range of 1–4 Hz, which precludes imaging of optical events of ~1 ms in duration. In contrast, wide-field imaging with high-speed CCD cameras or photodiode arrays can acquire images at rates >1 kHz (5). High-speed multiphoton scanning microscopes based on resonant galvanometers (16, 49) or acousto-optic deflectors (24, 36) can also scan individual lines (but not full frames) at speeds in the range of 7–16 kHz. However, line scanning samples only a tiny fraction of the field, removing much of the advantage of imaging over electrodes. The development of microscopes with random beam addressability in two dimensions, which are capable of scanning tens of locations at >1 kHz (22, 39), partially overcomes this limitation. It has also been demonstrated that it is possible to perform optical sectioning under special wide-field multiphoton illumination conditions (31). Nevertheless, scanning speed is a significant limitation for the vast majority of existing laser scanning microscopes.

The second, more fundamental, drawback of scanning microscopy is that the total number of photons detected in a given time interval is small relative to wide-field imaging. For example, Baker et al. (5) observe a 1,000-fold decrease in the number of photons collected using two-photon microscopy relative to wide-field microscopy under similar conditions. This is for two reasons. First, the excitation beam illuminates each point in the image only once per frame, whereas in wide-field imaging each point is illuminated continuously. Additionally, wide-field imaging collects light from an entire cell, not just a single plane through the cell. The effect of low photon flux on AP detection can best be quantified from the standpoint of signal detection theory.

Signal Detection Theory

Imaging experiments generally fall into two categories: parameter estimation and signal detection (32). In parameter estimation, single or multiple trials are used to estimate a specific parameter of the signal,

such as the amplitude of a calcium transient. Signal detection, on the other hand, deals with the detection of stereotyped events in noisy single trial data. Optical recording of APs from multiple cells is a problem of signal detection, since one is interested in detecting when events occur rather than measuring the exact waveform of each individual event. In this case, there are two possibilities at each time point: H_0, the null hypothesis, is that no AP occurred; and H_1, the alternative hypothesis, is that an AP did occur. To determine which hypothesis is correct, one examines the number of photons (x) per time bin collected from an imaging experiment. This is formalized in the likelihood functions, $P(x|H_0)$ and $P(x|H_1)$, which are the conditional probability distributions for a photon count of x in the absence or presence of an AP, respectively (FIGURE 2). $P(x|H_0)$ is the "noise" distribution, whereas $P(x|H_1)$ can be referred to as the "signal + noise" distribution. Based on each measurement of x, a decision is made: either D_0 (AP not detected), or D_1 (AP detected). At each time point, there are then four possible outcomes: (D_0,H_0) and (D_1,H_1) are both correct outcomes (no AP detected when no AP occurred; AP detected when AP occurred), whereas (D_1,H_0) is the type II error or "false positive" (AP detected when no AP occurred) and (D_0,H_1) is the type I error or "detection failure" (no AP detected when AP occurred). In the absence of noise (FIGURE 2A), the likelihood functions $P(x|H_0)$ and $P(x|H_1)$ are narrowly peaked without overlap, and simple thresholding can detect APs with perfect accuracy. However, in the presence of noise, the likelihood functions broaden and overlap (FIGURE 2B), and a trade-off is forced between detection failures and false positives. Signal detection theory provides methods for optimizing the detection efficiency, while holding false positives to an acceptable level.

The most fundamental noise source is photon shot noise, which reflects the quantal nature of light and the probabilistic nature of photon detection. For example, if a detector registers 10^6 photons per second (toward the low end of a typical laser scanning microscopy experiment) and each time bin is 1 ms in length (the duration of our model AP), each bin will contain 1,000 photons on average. However, by random chance, some bins will contain more than 1,000 photons and some will contain less. This statistical variation is known as shot noise, and it is the dominant noise source under low-light conditions. Statistically, photon collection is a Poisson process, and the number of photons x per time bin is distributed as

$$P(x \mid H_0) = \frac{\lambda^x e^{-\lambda}}{x!} \approx p(x \mid H_0) = \frac{1}{\sqrt{2\pi\lambda}} \exp\left(\frac{-(x-\lambda)^2}{2\lambda}\right)$$

where λ is the mean number of photons in each bin. The right side invokes the central limit theorem, which states that when λ is large, the Poisson distribution can be approximated as a Gaussian, or normal, distribution with a mean of λ and a standard deviation of $\sqrt{\lambda}$. For experimentally realistic values of λ, the Gaussian approximation is accurate, and we therefore adopt it for convenience.

To illustrate the effect of shot noise on signal detection, consider the simple case where an AP causes a voltage reporter to increase fluorescence by 10% for 1 ms. If each 1-ms bin contains 1,000 photons on average when no AP occurs, bins containing APs will contain 1,100 photons on average. Revisiting our fictitious zero-noise example (FIGURE 2A), we find it is easy to set a threshold that distinguishes an AP with perfect accuracy. Taking shot noise into consideration (FIGURE 2B), we see that the "noise" and "signal + noise" distributions overlap. As a consequence, it is no longer possible to achieve perfect detection efficiency with no false positives: an acceptable tradeoff must be determined. Since we do not know in advance how many APs to expect, the simplest criterion to guide us is the Neyman-Pearson decision rule (48). This decision rule sets a threshold to distinguish between bins containing APs and those not containing APs. If the number of photons in a bin is greater than this threshold, we decide an AP has occurred (D_1). The threshold is set arbitrarily to the level of false positives deemed acceptable, with increasing false positives leading to increased detection probability. For example, if we are willing to tolerate 10 spurious APs per second, a large number, the "false-positive" probability (P_{FP}) is 10^{-2} (10 out of the 1,000 1-ms time bins/s will contain a spurious AP). From the "noise" distribution $p(x \mid H_0)$, the threshold t is determined such that the area under the part of the curve falling above the threshold is equal to 10^{-2} (red region, FIGURE 2B). In this case,

$$P_{FP} = \int_t^\infty p(x \mid H_0)dx = 1 - \phi\left(\frac{t-\lambda_n}{\sqrt{\lambda_n}}\right) = 10^{-2}$$

$$t = \sqrt{\lambda_n}\phi^{-1}(1 - P_{FP}) + \lambda_n = 1{,}074 \text{ photons}$$

where ϕ is the standard normal cumulative distribution function. If more than 1,074 photons were detected, we decide an AP has occurred. Working with this threshold, the probability of successful AP detection (P_D) can be calculated from the "signal + noise" distribution $p(x \mid H_1)$ as the area under the curve to the right of the threshold (green region, FIGURE 2B):

$$P_D = \int_t^\infty p(x \mid H_1)dx = 1 - \phi\left(\frac{t-\lambda_{sn}}{\sqrt{\lambda_{sn}}}\right) = 0.78$$

In this case, shot noise limits detection to only 78% of APs, despite the high false-positive rate of 10 APs/s. If the cell were firing at 10 Hz, ~8 (out of 10) real APs/s would be detected along with 10 spurious ones. In other words, <45% of the APs detected would correspond to real APs, and we would overestimate the

neuron's true firing rate of 10 Hz by almost twofold as 18 Hz. These significant errors are a direct and unavoidable consequence of a low photon count; if the photon count increases, the situation improves dramatically, as discussed below.

There are other experimental noise sources in addition to shot noise, such as photodetector excess noise and power fluctuations in the excitation light source, but these can often be minimized, whereas shot noise is a fundamental limitation. Another simplification in this model is that, in practice, APs are usually oversampled such that a single AP is spread out over several time bins. Based on the expected waveform of the AP, a matched filter can be constructed to extract APs optimally. This approach will yield improved performance for real APs, which are not square pulses, but it does not circumvent the fundamental effect of shot noise on detection efficiency.

Signal Detection Model of Voltage Reporters

Taking the above considerations into account, it is instructive to describe a simple model of AP detection using voltage reporters with laser scanning microscopy. For all reporters, the fluorescence detected can be broken down into three functionally distinct pools (FIGURE 3). F_{PM} represents the plasma membrane fluorescence due to the voltage reporter. Because only plasma membrane-associated fluorophores are affected by the transmembrane electric field, F_{PM} is the only voltage-sensitive pool. F_{NS}, or nonspecific background fluorescence, is due to exogenous fluorophore that is not localized to the plasma membrane. Primary sources of F_{NS} include fluorophore in the cytoplasm or extracellular space, fluorophore associated with intracellular membranes, and fluorophore associated with nonneuronal cells and acellular tissue. The third fluorescence pool, B, is background fluorescence not due to exogenous fluorophore. The primary sources are endogenous tissue fluorophores and, to a lesser extent, inelastic light scattering and fluorescence of lens materials. We therefore have five parameters to consider when evaluating a voltage reporter: *1*) response kinetics, *2*) voltage sensitivity ($\delta F_{PM}/F_{PM}$), *3*) absolute brightness (F_{PM}), *4*) labeling specificity (F_{PM}/F_{NS}), and *5*) cellular perturbation.

We will analyze these parameters using a simplified model of AP detection with the Neyman-Pearson rule (FIGURE 4). Based on this model, we describe the relative importance of the five parameters in general and also in the context of specific voltage reporters.

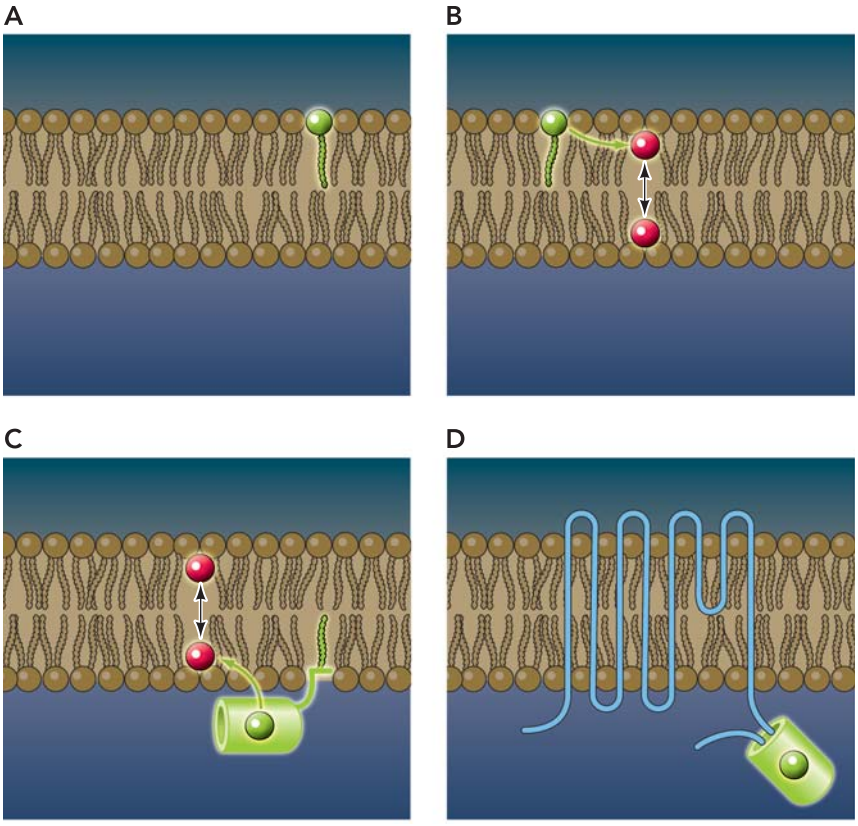

FIGURE 1. **Voltage-sensitive optical reporters**
A: in fast VSDs, the transmembrane electric field affects the dye molecule directly. *B*: in two-component VSDs, changes in membrane potential cause the mobile dye molecule to translocate from one leaflet of the membrane to the other. This alters the distance between the two dye populations and, therefore, the FRET efficiency between them. *C*: hybrid GFP-dye systems operate according to the same principle, with the stationary dye molecule replaced with a membrane-anchored GFP. *D*: in GFP-channel fusions, the channel undergoes voltage-dependent conformational changes that are translated to changes in GFP fluorescence.

Response kinetics

The issue of response kinetics is typically framed as whether the sensor is fast enough to follow an AP. In the context of high-speed wide-field imaging, it may indeed be appropriate to have a sensor with the fastest possible kinetics. With scanning microscopy, however, this is not necessarily the case. First, an optical event 1 ms in duration must be sampled at >1 kHz to be detected reliably. As noted previously, many systems are not capable of line scanning at this speed, and even for high-speed or random access scanning, the number of points that can be sampled depends on the duration of the individual optical event: to avoid detection failures while "looking elsewhere," each location has to be revisited at intervals shorter than the duration of a typical event. Short events require frequent revisits and thus limit the number of points that can be surveyed. Second, short events have few photons associated with them, making detection statistics less favorable. Since, for many applications, we are interested only in when APs occur, not in the detailed waveform of each AP, the relevant parameter is not the width of the AP but the mean interspike interval. An ideal sensor for scanning microscopy would have asymmetrical kinetics where the "on" kinetics are fast relative to the AP width and the "off" kinetics are slower but still fast relative to the mean interspike interval, so that individual spikes can be distinguished.

A simple version of this can be modeled by increasing *W*, the duration or width of the optical signal associated with the AP in the hypothetical case considered previously (FIGURE 2). FIGURE 4B shows that increasing the duration of the optical event dramatically increases detection efficiency. Increasing the duration of the optical signal is tantamount to enhancing the brightness of the indicator, since both increase the number of photons collected per AP, decreasing the effect of shot noise.

The response kinetics of fast VSDs are faster than the kinetics of APs themselves (12, 41). However, the response kinetics of two-component VSDs and hybrid GFP-dye systems are variable. High hydrophobicity of the mobile dye tends to correlate with fast kinetics (19), but hydrophobic dyes are harder to load into tissue (9). Nevertheless, some mobile dyes are sufficiently fast for AP recording. In the two-component VSD case, the use of highly hydrophobic versions of the mobile oxonol dye decreased the time constant to 0.4 ms, while in the hybrid GFP-dye case, the use of the hydrophobic quenching molecule dipicrylamine (DPA) yielded a time constant of 0.53 ms. In all cases, there is no mechanism for asymmetric kinetics, which makes APs more difficult to detect.

GFP-channel fusions are unique among voltage reporters in that the voltage-dependent conformational changes of voltage-gated cation channels exhibit hysteresis as a result of inactivation (2). In other words, a channel goes through a sequence of states on cell depolarization, but on repolarization the channel does not run through the same sequence in reverse but rather goes through a different set of states. This provides a potential biophysical substrate for the asymmetric on/off kinetics exhibited by the ideal voltage reporter. In practice, SPARC (3) and VSFP1 (38) show symmetric, sub-millisecond kinetics similar to VSDs. FlaSh, however, displays asymmetric responses to voltage pulses with an "on" time constant of ~23 ms and an "off" time constant of ~105 ms (43). Although this is too slow for AP recording, improved versions of FlaSh have "on" time constants as low as 9.7 ms (21), and it is possible that future versions of FlaSh will have even faster kinetics.

Voltage sensitivity ($\Delta F_{PM}/F_{PM}$)

Voltage sensitivity is typically reported in terms of measured ΔF/F per 100 mV, determined under wide-field illumination in cultured cells, *Xenopus* oocytes, or squid axons. This measurement corresponds to $\Delta F_{PM}/(F_{PM} + F_{NS} + B)$, which is necessarily an underestimate of $\Delta F_{PM}/F_{PM}$, the true voltage sensitivity of the voltage reporter, as the "nonproductive" terms F_{NS} and B also add to the denominator. Higher $\Delta F_{PM}/F_{PM}$ is always better, but the important point is that the $\Delta F_{PM}/F_{PM}$ necessary for efficient AP detection is highly dependent on the other parameters.

The voltage sensitivity of VSDs ranges up to 23% ΔF/F per 100 mV in cultured cells (35), although excitation of the red edge of the absorption spectrum of some dyes has been shown to increase this range to 70% ΔF/F per 100 mV (23) at the expense of a reduced total photon count. VSDs that give fast voltage-dependent SHG signals, such as FM4-64, yield lower sensitivity of up to 12% ΔF/F per 100 mV (37), but the SHG signal is generated selectively by membrane-bound dye molecules, decreasing F_{NS} and increasing measured ΔF/F in intact tissue. However, it should be noted that the SHG signal is collected not by the objective, but by a detector placed on the opposite side of the specimen, limiting applicability to a subset of intact tissue preparations. Two component VSDs based on coumarin-oxonol FRET pairs yield high sensitivity (up to 80% ΔF/F per 100 mV) for slowly responding oxonols, but oxonols fast enough for AP recording yield lower sensitivities of ~8% ΔF/F per 100 mV (19). The EGFP-DPA FRET pair in the hVOS system exhibits a comparably larger ΔF/F of up to 34% per 100 mV (10).

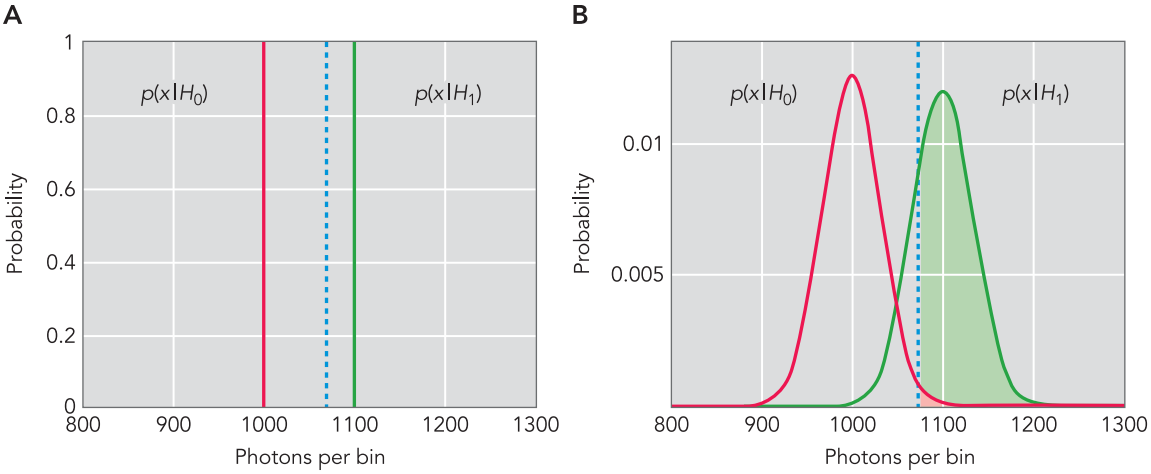

FIGURE 2. **Noise and signal + noise distributions**
A: in the fictitious zero-noise condition, the noise and signal + noise distributions do not overlap, and thresholding can distinguish with perfect accuracy. *B*: when photon shot noise is included, the distributions overlap. The threshold must be adjusted to balance false positives (red area) vs. detection efficiency (green area).

In GFP-channel fusions, each fluorescent molecule senses membrane voltage with multiple gating charges. As a result, GFP-channel fusions are theoretically capable of the greatest voltage sensitivity. In practice, however, GFP-channel fusions exhibit some of the lowest voltage sensitivities, in the range of <5% ΔF/F per 100 mV. This is an area for great improvement in this class of voltage reporters, since wild-type GFP exhibits low conformational sensitivity due to the rigid β-barrel structure shielding the chromophore (33). It is likely that the use of GFP variants with increased conformational sensitivity could greatly increase voltage sensitivity.

Absolute brightness (F_{PM})

The total photon flux a fluorophore can generate is one of the most important factors in practical imaging, and voltage reporters are no exception. There are two reasons for this. First, minimizing the relative contribution of background fluorescence B to total fluorescence increases the measured fractional fluorescence change $\Delta F_{PM}/(F_{PM} + F_{NS} + B)$. More importantly, photon shot noise scales as the square root of total photon number, i.e., decreases in relative importance as the photon count increases. Optical recording of APs in intact tissue involves short temporal windows and single-cell resolution, which usually requires laser scanning microscopy. As a result, the number of photons per AP is already low, and voltage reporters generating low numbers of photons can make AP detection very inefficient, if not impossible.

Evaluating the example of AP detection with a false-positive rate $P_{FP} = 10^{-4}$ and an AP lasting 1 ms (FIGURE 4D), we see that detection efficiency drops off precipitously below 3,000 photons per AP, or 3×10^6 photons per second. Although typical laser scanning microscopy experiments with some voltage reporters can generate $>10^7$ photons/s from a single cell, this has not been demonstrated with all voltage reporters. Despite great practical importance, there is no standard method for measuring or reporting brightness of voltage reporters. In theory, the brightness of a fluorophore could be quantified by taking into account the number of fluorophore molecules per cell, extinction coefficient (or two-photon absorption cross section), and quantum yield. In practice, however, fluorescence intensity is dependent on the power of the excitation light source, so photobleaching and phototoxicity become the limiting factors. With VSDs, this is usually the case.

One significant advantage of GFP-based voltage reporters is that GFP tends to have decreased photobleaching and phototoxicity relative to small molecule dyes. This is likely due to the β-barrel structure of GFP, which shields the chromophore from molecular oxygen (33). In addition, VSDs are in direct contact with membrane lipids, leading to lipid peroxidation (18), whereas the GFP of genetically encoded voltage reporters usually protrudes into the juxtamembrane cytoplasmic space, where the cell is less vulnerable to oxidative stress.

However, brightness is a significant problem with GFP-channel fusions, since incorporation of GFP into the channel protein typically decreases GFP folding efficiency severely (4). High absolute brightness is among the advantages of the hVOS GFP-dye system (10). Unlike GFP-channel fusions, in which the GFP must fold within the topological constraints of an integral membrane protein and reach the plasma membrane via transport through the secretory pathway, the prenylated EGFP-F fluorophore in hVOS is expressed as a soluble protein and membrane-targeted via post-translational lipidation (10, 36). As a result, each cell tends to produce more properly folded GFP molecules, resulting in more favorable photon statistics.

Nonspecific labeling (F_{NS}/F_{PM})

One of the primary differences between VSD performance in cultured cells and thick tissue specimens is due to nonspecific labeling. Nonspecific labeling arises from multiple sources, including VSD binding to nonexcitable cells and acellular tissue, or GFP molecules not localized to the plasma mem-

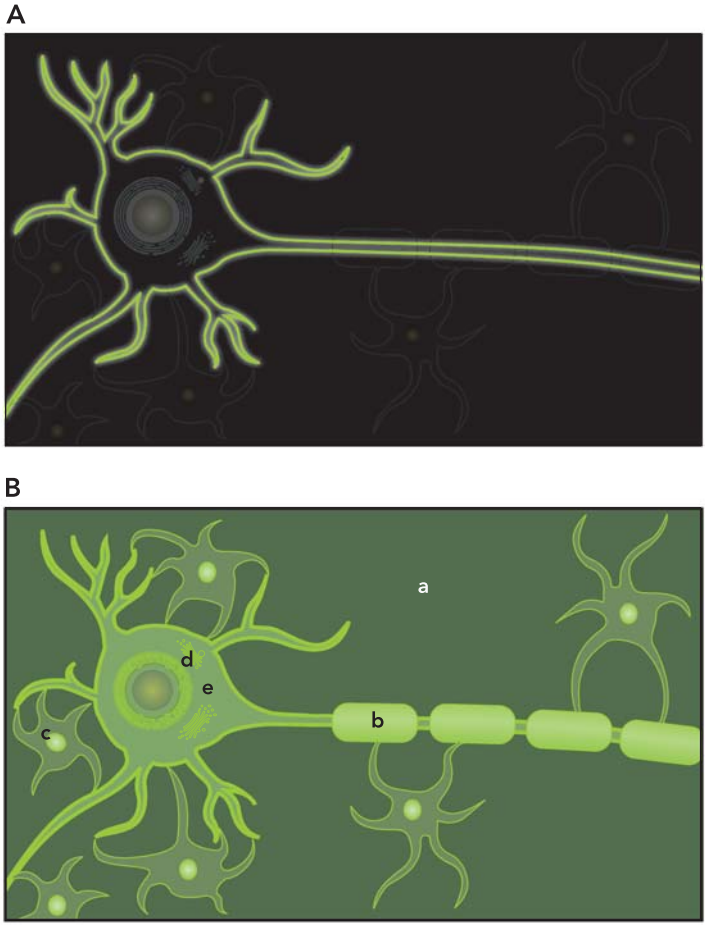

FIGURE 3. **Functionally distinct sources of fluorescence**
A: the ideal situation. Only fluorescent molecules localized to the plasma membrane (FPM) are voltage-sensitive. *B*: the real situation. Sources of noise include background fluorescence B (a) as well as nonspecific fluorescence FNS resulting from dye bound to non-neuronal cells (b and c) and GFP localized to intracellular organelles (d) and the cytoplasm (e).

brane. An ideal voltage reporter would have an F_{NS}/F_{PM} of zero, as any increase in F_{NS}/F_{PM} acts to decrease the effective $\Delta F/F$. FIGURE 4D shows that increases in F_{NS} lead to a significant decrease in detection efficiency.

The greatest drawback of VSDs is limited labeling specificity. Since the dyes are nonselectively added to the tissue, nonneuronal cells and acellular tissue are also labeled, increasing background fluorescence dramatically. The use of SHG, rather than fluorescence, with VSDs largely eliminates the nonspecific background, as only membrane-associated VSD molecules generate an SHG signal.

GFP-based voltage reporters are often believed to have superior labeling specificity, but this is not always the case. Although expression is limited to a particular cell population, not all of the fluorescent GFP molecules are localized to the plasma membrane. GFP-channel fusions, for example, are translated in the rough ER and transported through the secretory pathway. Usually, significant amounts of GFP fluorescence are retained in the ER and Golgi (4). This may reflect quality control mechanisms preventing the export of channels that are misfolded due to GFP insertion, physiological control of channel densities on the cell surface, or both.

High membrane specificity is one of the great strengths of the hVOS system (10). Unlike GFP-channel fusions, the GFP is expressed as a soluble protein and posttranslationally targeted to the plasma membrane (10, 36). As a result, a significantly higher fraction of total GFP molecules are localized to the plasma membrane relative to GFP-channel fusions.

Cellular perturbation

Although not explicitly linked to the other parameters, the extent to which a voltage reporter perturbs normal cellular function also places limits on its utility. For example, VSDs are known to sensitize cells to photodamage, limiting the duration for which preparations can be illuminated and observed (12).

A more important, underappreciated perturbation is the increased capacitive load that results from adding mobile "probe" charges to sense the transmembrane potential. The additional capacitive load of fast VSDs is insignificant, but it is a problem in the context of two-component VSDs and hybrid GFP-dye systems (9, 10, 19, 20), where the movement of the mobile dye molecule has been shown to inhibit APs at high concentrations (10). The problem of capacitive load is most severe with GFP-channel fusions, as voltage-gated cation channels typically possess 12–14 gating charges per channel (1, 42), leading to a steeper voltage dependence of charge movement and a higher capacitive load per mobile charge. The ratio of GFP molecules to mobile charges is also unfavorable from a signal detection standpoint. For example, if a GFP-channel fusion protein containing one GFP per channel tetramer is expressed at a level of 23,000 charges per μm^2, which is typical for these experiments (7), then there are ~1,800 GFP molecules per μm^2 of membrane. For a spherical cell of 20-μm diameter, the number of GFP molecules per cell is less than if the cell's cytoplasm were filled with 1 μM GFP, the concentration at which GFP fluorescence equals cellular autofluorescence (29). Imaging a planar membrane containing 1,800 GFPs/μm^2 with two photon microscopy, the GFP concentration inside the excitation volume (calculated as in Ref. 51) equals ~1 μM. Two-photon excitation of 1 μM GFP with 15 mW of laser power yields ~10^6 photons/s, which is a borderline value for detecting APs with a voltage sensor

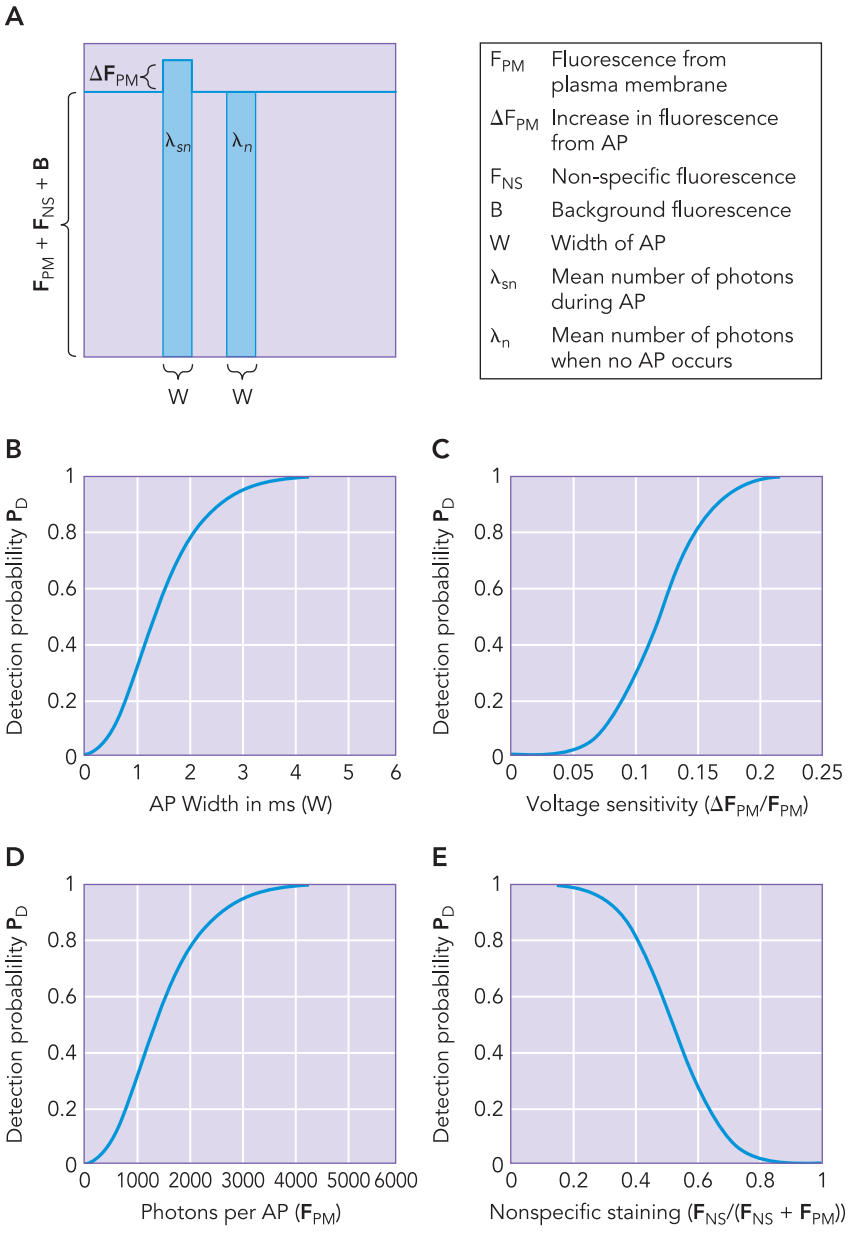

FIGURE 4. **Signal detection model of optical AP detection**
A: description of model. Default parameters: false positive probability (P_{FP}) = 10^{-4}, λ_n = 1,000 photons, and λ_{sn} = 1,100 photons. *B*: increasing the temporal width of the response to an AP increases detection probability (P_D). *C*: increasing voltage sensitivity $\Delta F_{PM}/F_{PM}$ increases detection probability (P_D). *D*: increasing fluorescence intensity F_{PM} increases P_D. *E*: increasing nonspecific labeling decreases P_D.

reporting APs with a 10% increase in fluorescence (FIGURE 4, C AND D). Inefficient folding or maturation of GFP in the context of an ion channel fusion protein will, of course, further diminish the expected photon flux. Despite these low fluorescence levels, the addition of 23,000 mobile charges per μm^2 increases the membrane capacitance by ~370%, which is far above the level shown to inhibit APs in vitro (10). As a result, capacitive load places severe restrictions on expression level and fluorescence yield of GFP-channel fusion proteins.

Although hVOS also increases membrane capacitance, the problem is less severe because GFP fluorescence quenching will occur even if there is less than one DPA molecule per GFP, since only a fraction of the GFP molecules are in the excited state at any given time. As a result, there is a much smaller capacitive load per GFP molecule, yielding a brighter signal with less perturbation to normal cellular function.

Conclusion

Imaging physiological signals in intact tissue creates opportunities as well as challenges. Laser scanning microscopy enables high-resolution imaging in scattering tissue at the cost of low photon counts, which render AP detection in single trials difficult except in the most favorable of circumstances (37). To do better than an electrode, the goal of all optical approaches must be to record not the activity of a single neuron but of many neurons simultaneously. To reach this goal, the efficiency of every level in the process must be improved dramatically: faster scanning (22, 39), more efficient photon collection (46), greater depth penetration (44), and the ability to sample predefined locations rapidly in three dimensions (34). Progress is being made on all fronts, but the ideal type of microscopy for this purpose has yet to be demonstrated.

There is also significant room for improvement in voltage-sensitive reporter molecules, in particular those with a genetically encodable component. In designing such probes, it is wise to compare carefully the photon fluxes expected from a voltage reporter with those needed to detect an AP in a single trial. Such an analysis will take into account the brightness of individual molecules, the densities at which they can be inserted into the plasma membrane without disrupting normal physiology, the size of the membrane patch surveyed in a typical experiment, the voltage sensitivity and response kinetics of the probe, and the specificity of cell surface labeling. A VSD pioneer remarked that "in some fields one can be reasonably certain that [a given] path will bear fruit; if not in one's own laboratory, at least in other laboratories pursuing the same subject. . . . [But in other fields] it may be generations or centuries before it is known whether a chosen path was fruitful. The risk of devoting one's life to a dead end does lend excitement to the choice (11)." Keeping the principles of signal detection theory in mind should allow one to minimize this risk. ■

We thank Larry Cohen for comments.

Work in the authors' laboratory is supported by the National Institutes of Health, Office of Naval Research, and the W. M. Keck Foundation.

References

1. Aggarwal SK, MacKinnon R. Contribution of the S4 segment to gating charge in the Shaker K+ channel. *Neuron* 16: 1169–1177, 1996.
2. Armstrong CM, Bezanilla F. Inactivation of the sodium channel. II. Gating current experiments. *J Gen Physiol* 70: 567–590, 1977.
3. Ataka K, Pieribone VA. A genetically targetable fluorescent probe of channel gating with rapid kinetics. *Biophys J* 82: 509–516, 2002.
4. Baker BJ, Cohen LB, Pieribone VA, Kosmidis EK. Expression of the GFP-voltage sensor SPARC in HEK 293 cells (Abstract). *Biophys J* 86: 425, 2004.
5. Baker BJ, Kosmidis EK, Vucinic D, Falk CX, Cohen LB, Djurisic M, Zecevic D. Imaging brain activity with voltage- and calcium-sensitive dyes. *Cell Mol Neurobiol* 25: 245–282, 2005.
6. Betz WJ, Bewick GS. Optical analysis of synaptic vesicle recycling at the frog neuromuscular junction. *Science* 255: 200–203, 1992.
7. Bezanilla F, Perozo E, Stefani E. Gating of Shaker K+ channels: II. The components of gating currents and a model of channel activation. *Biophys J* 66: 1011–1021, 1994.
8. Bouevitch O, Lewis A, Pinevsky I, Wuskell JP, Loew LM. Probing membrane potential with nonlinear optics. *Biophys J* 65: 672–679, 1993.
9. Cacciatore TW, Brodfuehrer PD, Gonzalez JE, Jiang T, Adams SR, Tsien RY, Kristan WB Jr, Kleinfeld D. Identification of neural circuits by imaging coherent electrical activity with FRET-based dyes. *Neuron* 23: 449–459, 1999.
10. Chanda B, Blunck R, Faria LC, Schweizer FE, Mody I, Bezanilla F. A hybrid approach to measuring electrical activity in genetically specified neurons. *Nat Neurosci* 8: 1619–1626, 2005.
11. Cohen LB. Risk and pleasure [Online]. Yale University. http://infomedyaleedu/cmphysiol/education/graduate/Perspectives/Cohen.html.
12. Cohen LB, Salzberg BM. Optical measurement of membrane potential. *Rev Physiol Biochem Pharmacol* 83: 35–88, 1978.
13. Davila HV, Salzberg BM, Cohen LB, Waggoner AS. A large change in axon fluorescence that provides a promising method for measuring membrane potential. *Nat New Biol* 241: 159–160, 1973.
14. Denk W, Strickler JH, Webb WW. Two-photon laser scanning fluorescence microscopy. *Science* 248: 73–76, 1990.
15. Dragsten PR, Webb WW. Mechanism of the membrane potential sensitivity of the fluorescent membrane probe merocyanine 540. *Biochemistry* 17: 5228–5240, 1978.
16. Fan GY, Fujisaki H, Miyawaki A, Tsay RK, Tsien RY, Ellisman MH. Video-rate scanning two-photon excitation fluorescence microscopy and ratio imaging with cameleons. *Biophys J* 76: 2412–2420, 1999.
17. Fromherz P, Lambacher A. Spectra of voltage-sensitive fluorescence of styryl-dye in neuron membrane. *Biochim Biophys Acta* 1068: 149–156, 1991.
18. Girotti AW. Photosensitized oxidation of membrane lipids: reaction pathways, cytotoxic effects, and cytoprotective mechanisms. *J Photochem Photobiol B* 63: 103–113, 2001.
19. Gonzalez JE, Tsien RY. Improved indicators of cell membrane potential that use fluorescence resonance energy transfer. *Chem Biol* 4: 269–277, 1997.
20. Gonzalez JE, Tsien RY. Voltage sensing by fluorescence resonance energy transfer in single cells. *Biophys J* 69: 1272–1280, 1995.

21. Guerrero G, Siegel MS, Roska B, Loots E, Isacoff EY. Tuning FlaSh: redesign of the dynamics, voltage range, and color of the genetically encoded optical sensor of membrane potential. *Biophys J* 83: 3607–3618, 2002.

22. Iyer V, Hoogland TM, Saggau P. Fast functional imaging of single neurons using random-access multiphoton (RAMP) microscopy. *J Neurophysiol* 95: 535–545, 2006.

23. Kuhn B, Fromherz P, Denk W. High sensitivity of Stark-shift voltage-sensing dyes by one- or two-photon excitation near the red spectral edge. *Biophys J* 87: 631–639, 2004.

24. Lechleiter JD, Lin DT, Sieneart I. Multi-photon laser scanning microscopy using an acoustic optical deflector. *Biophys J* 83: 2292–2299, 2002.

25. Loew LM, Cohen LB, Salzberg BM, Obaid AL, Bezanilla F. Charge-shift probes of membrane potential. Characterization of aminostyrylpyridinium dyes on the squid giant axon. *Biophys J* 47: 71–77, 1985.

26. Miesenbock G, De Angelis DA, Rothman JE. Visualizing secretion and synaptic transmission with pH-sensitive green fluorescent proteins. *Nature* 394: 192–195, 1998.

27. Miesenbock G, Kevrekidis IG. Optical imaging and control of genetically designated neurons in functioning circuits. *Annu Rev Neurosci* 28: 533–563, 2005.

28. Miyawaki A. Innovations in the imaging of brain functions using fluorescent proteins. *Neuron* 48: 189–199, 2005.

29. Niswender KD, Blackman SM, Rohde L, Magnuson MA, Piston DW. Quantitative imaging of green fluorescent protein in cultured cells: comparison of microscopic techniques, use in fusion proteins and detection limits. *J Microsc* 180: 109–116, 1995.

30. Obaid AL, Koyano T, Lindstrom J, Sakai T, Salzberg BM. Spatiotemporal patterns of activity in an intact mammalian network with single-cell resolution: optical studies of nicotinic activity in an enteric plexus. *J Neurosci* 19: 3073–3093, 1999.

31. Oron D, Tal E, Silberberg Y. Scanningless depth-resolved microscopy. *Optics Express* 13: 1468–1476, 2005.

32. Osche GR. *Optical Detection Theory for Laser Applications*. Hoboken, NJ: Wiley-Interscience, 2002.

33. Prendergast FG. Biophysics of the green fluorescent protein. *Methods Cell Biol* 58: 1–18, 1999.

34. Reddy GD, Saggau P. Fast three-dimensional laser scanning scheme using acousto-optic deflectors. *J Biomed Opt* 10: 064038, 2005.

35. Rohr S, Salzberg BM. Multiple site optical recording of transmembrane voltage (MSORTV) in patterned growth heart cell cultures: assessing electrical behavior, with microsecond resolution, on a cellular and subcellular scale. *Biophys J* 67: 1301–1315, 1994.

36. Roorda RD, Hohl TM, Toledo-Crow R, Miesenbock G. Video-rate nonlinear microscopy of neuronal membrane dynamics with genetically encoded probes. *J Neurophysiol* 92: 609–621, 2004.

37. Sacconi L, Dombeck DA, Webb WW. Overcoming photodamage in second-harmonic generation microscopy: real-time optical recording of neuronal action potentials. *Proc Natl Acad Sci USA* 103: 3124–3129, 2006.

38. Sakai R, Repunte-Canonigo V, Raj CD, Knopfel T. Design and characterization of a DNA-encoded, voltage-sensitive fluorescent protein. *Eur J Neurosci* 13: 2314–2318, 2001.

39. Salome R, Kremer Y, Dieudonne S, Leger JF, Krichevsky O, Wyart C, Chatenay D, Bourdieu L. Ultrafast random-access scanning in two-photon microscopy using acousto-optic deflectors. *J Neurosci Methods* 154: 161–174, 2006.

40. Salzberg BM, Davila HV, Cohen LB. Optical recording of impulses in individual neurones of an invertebrate central nervous system. *Nature* 246: 508–509, 1973.

41. Salzberg BM, Obaid AL, Bezanilla F. Microsecond response of a voltage-sensitive merocyanine dye: fast voltage-clamp measurements on squid giant axon. *Jpn J Physiol* 43, *Suppl* 1: S37–S41, 1993.

42. Seoh SA, Sigg D, Papazian DM, Bezanilla F. Voltage-sensing residues in the S2 and S4 segments of the Shaker K+ channel. *Neuron* 16: 1159–1167, 1996.

43. Siegel MS, Isacoff EY. A genetically encoded optical probe of membrane voltage. *Neuron* 19: 735–741, 1997.

44. Theer P, Hasan MT, Denk W. Two-photon imaging to a depth of 1000 microm in living brains by use of a Ti:Al2O3 regenerative amplifier. *Opt Lett* 28: 1022–1024, 2003.

45. Tsien RY, Gonzalez JE. Detection of transmembrane potentials by optical methods. In: *United States Patent*. Oakland, CA: The Regents of the University of California, 2002.

46. Vucinic D, Bartol TM Jr, Sejnowski TJ. Hybrid reflecting objectives for functional multiphoton microscopy in turbid media. *Opt Lett* 31: 2447–2449, 2006.

47. Waggoner AS, Grinvald A. Mechanisms of rapid optical changes of potential sensitive dyes. *Ann NY Acad Sci* 303: 217–241, 1977.

48. Whalen AD. *Detection of Signals in Noise*. New York: Academic Press, 1971.

49. Wiseman PW, Squier JA, Ellisman MH, Wilson KR. Two-photon image correlation spectroscopy and image cross-correlation spectroscopy. *J Microsc* 200: 14–25, 2000.

50. Zhang J, Campbell RE, Ting AY, Tsien RY. Creating new fluorescent probes for cell biology. *Nat Rev Mol Cell Biol* 3: 906–918, 2002.

51. Zipfel WR, Williams RM, Webb WW. Nonlinear magic: multiphoton microscopy in the biosciences. *Nat Biotechnol* 21: 1369–1377, 2003.